



Deformation banding in β working of two-phase TA15 titanium alloy

Xiao-guang FAN, Xiang ZENG, He YANG, Peng-fei GAO, Miao MENG, Rui ZUO, Peng-hui LEI

State Key Laboratory of Solidification Processing, School of Materials Science and Engineering,
Northwestern Polytechnical University, Xi'an 710072, China

Received 8 July 2016; accepted 8 December 2016

Abstract: To study deformation banding in β working of TA15 titanium alloy, hot simulation compression experiments were carried out on a Gleeble 3500 thermal simulator, and the microstructure was investigated by optical microscopy (OM) and electron back-scattered diffraction (EBSD). It is found that in β working of TA15 titanium alloy, deformation banding is still an important grain refinement mechanism up to temperature as high as $0.7T_m$ (T_m is the melting temperature). Boundaries of deformation bands (DBBs) may be sharp or diffusive. Sharp DBBs retard discontinuous dynamic recrystallization (DDRX) by prohibiting nucleation, while the diffusive ones are sources of continuous dynamic recrystallization (CDRX). Deformation banding is more significant at high strain rate and large initial grain size. The average width of grain subdivisions is sensitive to strain rate but less affected by temperature and initial grain size. Multi-directional forging which produces crossing DBBs is potential to refine microstructure of small-size forgings.

Key words: TA15 titanium alloy; β working; deformation banding; grain refinement; dynamic recrystallization

1 Introduction

Two-phase titanium alloy is widely used in many industry fields as a kind of lightweight structural material with high specific strength and good corrosion resistance. Hot working can tailor the microstructure along with shaping, which is one of the most applicable forming methods of titanium alloy. Generally, it contains deformation in both the single β region (β working) and the two-phase region. β working aims to refine the as-cast coarse β grains. With a finer β wrought structure, homogeneous microstructure can be obtained after subsequent deformation in the two-phase region. Therefore, the refinement of the β grains through hot working is crucial to the fabrication of titanium alloy component.

Deformation-induced grain refinement has long been recognized by researchers, and a lot of work has been carried out on the mechanism of microstructure refinement in β working of titanium alloys. Due to the high stacking fault energy (SFE) associated with the body centered cubic crystal structure as well as the high

deformation temperature in β working (usually higher than half of the melting temperature (T_m)), dynamic recovery (DRV) is considered to be the main restoration mechanism [1,2]. Thus, dislocation substructures are formed inside the original β grains [3,4]. Meanwhile, discontinuous dynamic recrystallization (DDRX) is also observed though it is greatly suppressed by strong DRV [5]. The recrystallized fraction is usually very limited. DING et al [6,7] reported a recrystallized fraction of less than 30% for Ti–6Al–4V alloy. Dynamic recrystallization (DRX) occurs more easily with the increase of deformation temperature and the decrease of strain rate [8,9]. Also, the recrystallization kinetics can be different from that of low SFE metals. DDRX is more significant at high deformation speed for a wide range of titanium alloys [10–13]. This phenomenon is interpreted in terms of the high stored energy at high strain rate which provides more driving force for the nucleation and growth of DDRX. WANG et al [14] reported a regular DDRX kinetics for a TC11 alloy. Meanwhile, the deformation banding may greatly affect DDRX and static recrystallization (SRX). It has been found that transition bands of the deformation bands (DBs) can serve as the

Foundation item: Projects (51205317, 51575449) supported by the National Natural Science Foundation of China; Project (50935007) supported by the National Natural Science Foundation of China for Key Program; Project (3102015AX004) supported by the Fundamental Research Funds for the Central Universities, China; Project (104-QP-2014) supported by the Research Fund of the State Key Laboratory of Solidification Processing, China

Corresponding author: Xiao-guang FAN; Tel: +86-29-88460212; E-mail: fxg3200@nwpu.edu.cn

DOI: 10.1016/S1003-6326(17)60265-6

nucleation site for recrystallization, so deformation banding may be used to modulate recrystallization. Instead of DDRX, for high SFE material, continuous dynamic crystallization (CDRX), geometric dynamic recrystallization (GDRX) and deformation banding induced grain subdivision are more important refining mechanisms [15]. They have been reported in hot working of some β and near- β titanium alloys [16,17]. TIAN et al [18] reported the transformation from DRV to CDRX with strain in hot deformation of Ti2448 alloy. CDRX in high temperature deformation of high SFE metals may originate from grain subdivision process.

DBs form at moderate and higher strain rates, which are the coarsest form of grain subdivision and play an important role in grain refinement. It is caused by local simultaneous operation of fewer slip systems to minimize the energy consumption and often accompanied by the inhomogeneous deformation inside grains [19]. The grain interior deforms on different slip systems, resulting in DBs with widely divergent orientations. The DB boundaries (DBBs) can be either sharp or diffusive [20]. The diffusive DBBs are referred to as transition bands. A smooth transition between the lattice orientations of adjacent deformation boundaries is accomplished over the thickness of the transition band [21]. With increasing strain, DBs may gradually evolve to high angle grain boundaries (HAGBs). The orientation changes continuously toward the grain boundaries.

Though deformation banding has been reported in β working of some titanium alloys, the effect of deformation banding on β grain refinement has not been clarified.

The purpose of the present work is to investigate the role of deformation banding and the related microstructural mechanisms in β working of two-phase titanium alloy and discuss their potential in grain refinement. This can be used to develop a feasible way for microstructure refinement in β working of two-phase titanium alloy.

2 Experimental

The material used in the current study was a near- α TA15 titanium alloy with measured chemical composition of Ti–6.69Al–2.25Zr–1.76Mo–2.25V–0.14Fe–0.12O and β -transus temperature of 1258 K. The as-received material was a hot forged bar with equiaxed structure. Cylinders of 15 mm in height and 10 mm in diameter were machined from the as-received bar and conducted for hot compression on a Gleeble 3500 thermal simulator. They were heated at a rate of 10 K/s to 100 K below the deformation temperature, then heated to the deformation temperature at 2 K/s, held for 15 min for

homogenization and deformed at the preset temperature and strain rate. During 2-pass compression, the cylinders were compressed along the radius direction at the same temperature and strain rate of the first compression which was compressed along the height direction, and water quenching was used to keep the microstructure of the first compression. The compression tests were performed at temperatures of 1293–1453 K, strain rates of 0.01–1 s⁻¹ to reduction rates of 20%–60% (In this work, the actual true strains were used. When the reduction rates were 20%, 40% and 60%, the corresponding average true strain were 0.27, 0.72 and 1.3, respectively). After deformation, the specimens were cooled in the air.

The microstructure was examined by optical microscopy (OM). The specimens were sectioned along the compression axis and prepared for metallurgical observation at the center of the specimens. Micrographs were taken on a Lecia DMI3000 microscope. The initial β grain size ranged from 300 to 500 μ m, as shown in Fig. 1(a). Additionally, the as-received material was annealed at 1473 K for 150 min to obtain coarse β grains whose grain sizes were about 1 mm, as shown in Fig. 1(b).

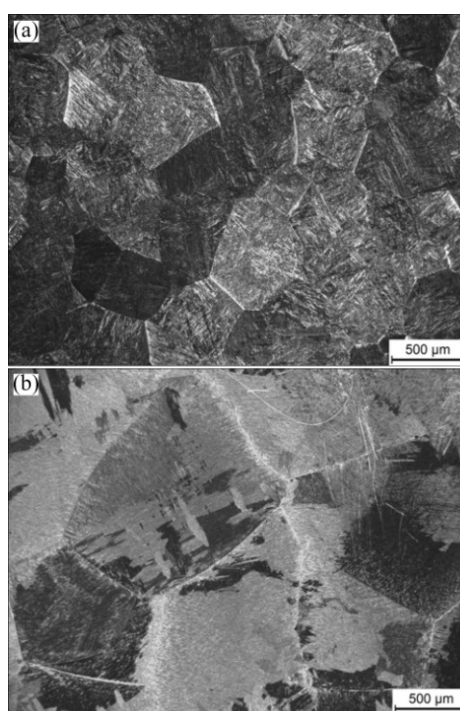


Fig. 1 Microstructures prior to deformation: (a) Directly heated to 1353 K and held for 15 min; (b) Annealed at 1473 K for 150 min

Electron back-scattered diffraction (EBSD) was used to examine the crystal orientation of the lamellar α and residual β phases. The air cooled specimen was reheated to 1173 K and held for 30 min to improve the

electron back-scattered pattern quality (In this work, the β phase was the point that we focused on, and the large number of lamellar α around the residual β phases would inhibit the SRX of few β phases, so this heat treatment had no influence on the precision of our results). Then, it was sectioned and mechanically ground on successive SiC papers to 2000 grit. Subsequently, it was electro-polished in a solution of 7% perchloric acid, 36% methanol and 57% *n*-butyl alcohol at 300 K (actual room temperature) and voltage of 22 V for 40 s. EBSD scans were carried out on a TESCAN MIRA3 XMU SEM equipped with an EBSD system developed by Oxford Instruments. A step size of 0.35 μm was used so that the residual β phases were identified, and the phase indexing rate reached 91%. The data were analyzed with the software Channel5.

3 Results and discussion

3.1 Flow stress curves

Figure 2 shows the stress–strain curves of the alloy at different temperatures and strain rates. Similar to other titanium alloys, the TA15 alloy also exhibits a high yield stress, rapid but limited working hardening at the early stage of β working, and the flow stress reaches a peak at the strain of 0.1–0.2. Then, a continuous softening occurs up to the strain of 0.5–0.8. This is followed by a plausibly additional hardening which is more significant at high strain rate. The additional hardening begins at strain around 0.6 and the hardening rate is comparable to the softening rate.

In the present work, the curves at the initial stage are DRV type in which flow stress gradually reaches the steady state with a small work hardening degree, while the subsequent softening is DDRX type where multi-peaks can be observed in the flow stress. This would result in contradiction, as the steady state flow stress may be lower than the initial yield stress (Fig. 2). So, the flow stress behavior may not be interpreted in

terms of traditional DDRX theory. In severe plastic deformation (SPD) of some high SFE metals, flow softening appears just after yielding and lasts until a very large strain [22,23]. Therefore, the shape of the flow stress curve at low strain rate is comparable to that in SPD. Grain boundary sliding and grain rotation may account for the flow stress drop. The softening at higher strain rate may have something to do with other microstructure phenomenon.

Another interesting phenomenon is the additional working hardening after flow softening. This is often caused by the texture evolution in hot working. Texture can be greatly changed by grain subdivision process, especially by deformation banding. Meanwhile, grain subdivision is driven by the reduction in consumed energy, which may cause softening.

3.2 Identification of DBs

The microstructure development at strain rate of 1 s^{-1} is illustrated in Fig. 3. It is found that some plausible boundaries firstly form near the initial β grain boundaries and spread into the grains, as indicated by the arrows in Fig. 3(a). These boundaries are about perpendicular to the compression axis or parallel to the initial grain boundaries. They also tend to appear in parallel pairs (indicated by blue and red arrows) and they are not the shear bands which extend to several grains. A series of neighbored plausible boundaries in parallel form are also observed (Fig. 3(b)). With increasing strain, narrow bands appear and split the grains, as demonstrated by red arrow in Fig. 3(c). The boundaries of the bands can be sharp, just like other HAGBs. On the other hand, there are additional bands with diffusive boundaries between the newly formed bands and the original grains (blue arrow in Fig. 3(c)), which may correspond to the transition bands. With larger strain, these boundaries are further sharpened (Fig. 3(d)) and they tend to be perpendicular to the compression axis. The original β grains are pancaked during deformation

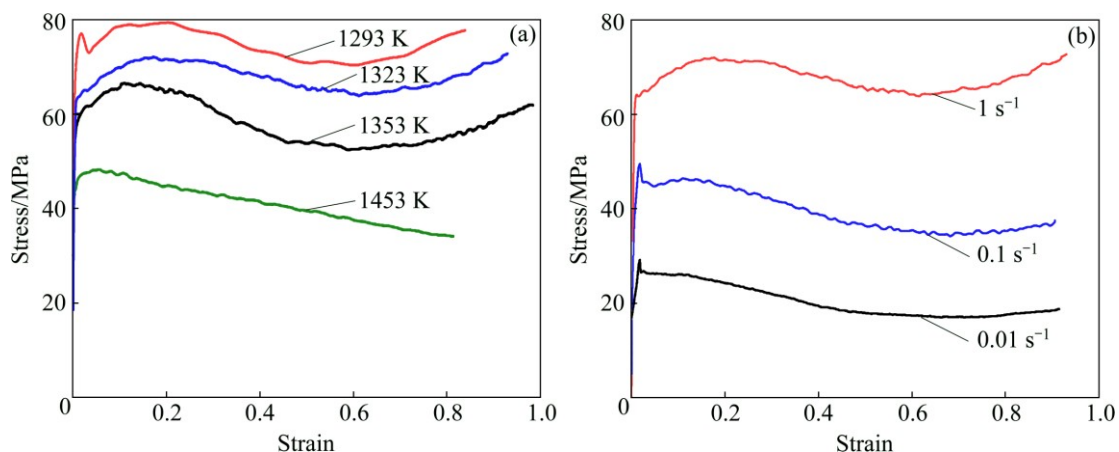


Fig. 2 Flow stress curves of alloy at different temperatures (a) and strain rates (b)

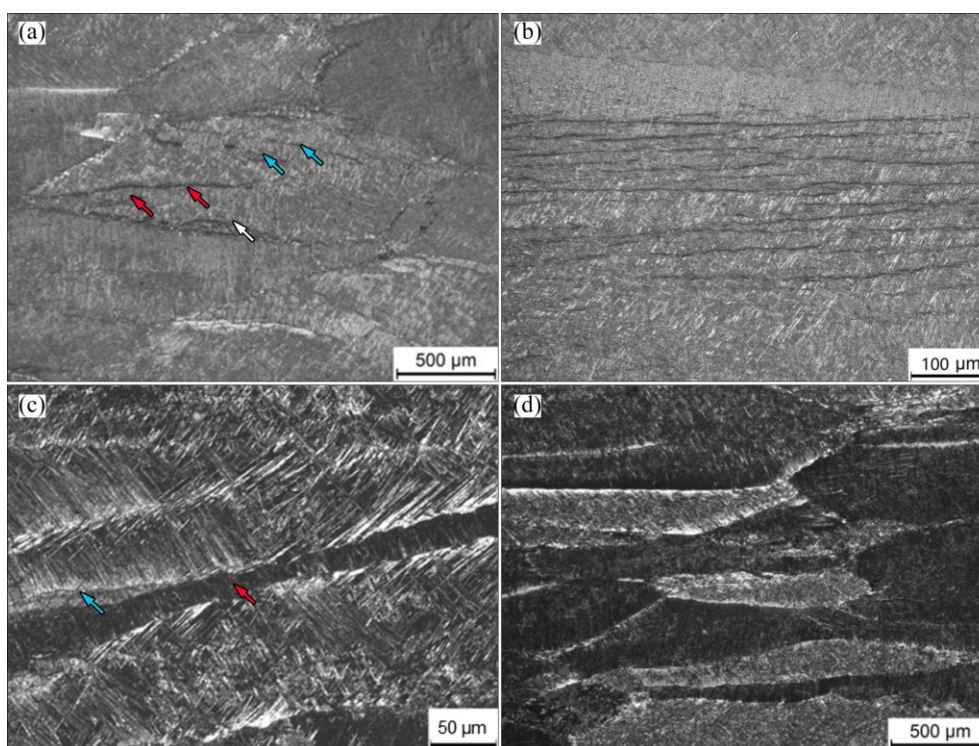


Fig. 3 Grain subdivision at different strains (The deformation temperature and strain rate are 1383 K and 1 s^{-1} , respectively. The compression axis is vertical herein and after): (a, b) 0.35; (c) 0.5; (d) 0.72

and further split by the newly formed boundaries. As a result, strip like β grains were obtained after deformation. Therefore, it may be deduced that deformation banding occurs in the present work.

To identify this phenomenon, the misorientation change in these bands is examined, and the measured zones are divided into several divisions by these boundaries, as shown in Figs. 4 and 5. The identified residual β phase is about 2% of the total. However, most of the residual β phase and the neighboring α phase follow the Burgers orientation relationship ($\{0001\}_{\alpha} // \{110\}_{\beta}$), as shown in the $\{110\}$ pole figure of β phase and the $\{0001\}$ pole figure of α phase (Fig. 4). At the same time, the inverse pole figures of α phase and β phase are given in Fig. 4. Thus, the data are applicable.

Based on the orientations of residual β phase detected by EBSD and the grain boundaries observed by optical microscope, the primary β phase is reconstructed and different colors stand for different orientations (the same as Fig. 4), as shown in Fig. 5. The corresponding orientations of residual β phase are shown in $\{100\}$ pole figures and the misorientation of the boundaries is measured.

The suspected boundaries are illustrated by red lines while the clear β grain boundaries are shown in black. In Fig. 5(a), A1 and B1 belong to different initial grains, so the orientation change is very sharp. From B1 to F1, the orientation change is more continuous, indicating the existence of transition bands. The average misorientation

angle between C1 and E1 is less than 10° , so does that between D1 and F1. Meanwhile, the misorientation angles for C1–D1 and E1–F1 are about 20° and 35° , respectively. This fulfills the definition of kink band in deformation banding, which involves a double orientation change A to C and then C to A [20]. A similar behavior is observed for D2–F2–G2–H2 in Fig. 5(b). The misorientation angle of these boundaries increases with the increase of strain. Meanwhile, the orientation change between different bands (E2–F2–G2–H2 in Fig. 5(b)) is so drastic that these boundaries are similar to HAGBs. HUGHES and HANSEN [24] reported that the misorientation angle of DBBs is often above 40° , which is higher than that of MSBs. The misorientation angle reaches 53° at the strain of 1.3 (F2–G2 and G2–H2). Thus, it is confirmed that deformation banding occurs in β working.

It is uncommon to observe DBs at temperatures as high as $0.7T_m$ [16]. HUMPHREYS and HATHERLY [20] summarized that deformation is more homogeneous at elevated temperatures, so deformation banding is suppressed. Large scale DBs were not found at strain as high as 1.4 when Al–0.3Mn was deformed at 673 K (about $0.72T_m$). KUHLMANN-WILSDORF et al [25] reported that DBs were very weak or absent at and above 473 K ($0.51T_m$) for Al–Cu–Si and Al–Cu alloys. In this work, DBs are observed at temperature of 1453 K (about $0.74T_m$) and strain of 0.72, as shown by the arrows in Fig. 6. The temperature is about 200 K above the β

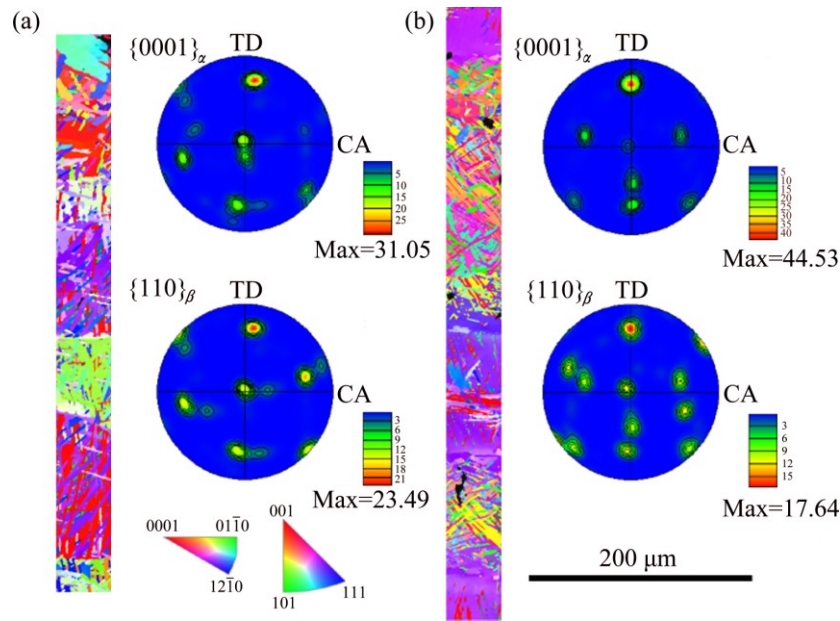


Fig. 4 Inverse pole figures and pole figures at strains of 0.72 (a) and 1.3 (b)

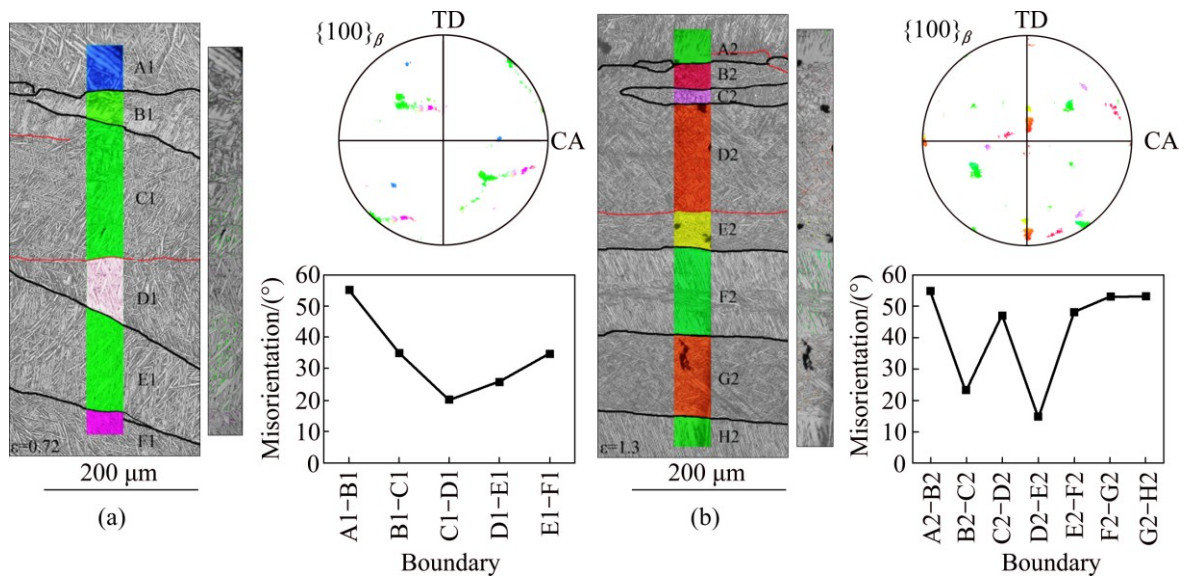


Fig. 5 Reconstructed primary β phase, inverse pole figures and $\{100\}$ pole figures of residual β phase and boundary misorientation at strains of 0.72 (a) and 1.3 (b)

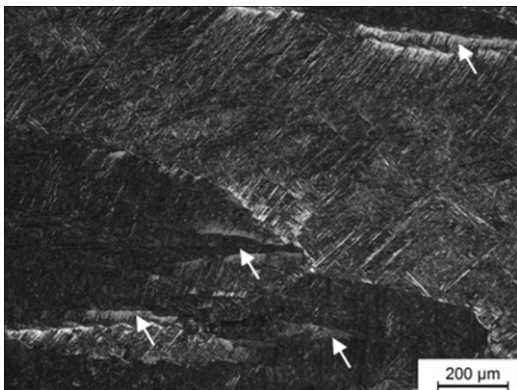


Fig. 6 DBs in specimen deformed at temperature of 1453 K, strain rate of 1 s^{-1} and strain of 0.72

transus temperature, which is the commonly highest deformation temperature in primary working of two-phase titanium alloys. This uncommon phenomenon may relate to different crystal structures.

3.3 Effect of processing on DBs

Deformation banding is sensitive to strain rate. In this work, DBs cannot be identified at strain rate of 0.01 s^{-1} because the deformation matrix is occupied by small equiaxed DDRX grains, as shown in Fig. 7. DDRX initiates at strain less than 0.2 under such strain rate. The recrystallized fraction can be as large as 50% at strain of 1.3 and even the lowest deformation temperature of 1293 K. Due to the strong dynamic restoration by DRV

and DDRX, the local hardening and stress concentration are greatly suppressed, so does the deformation banding.

DBs are found at strain rates above 0.1 s^{-1} . For specimens with initially small grain size ($300\text{--}500 \mu\text{m}$), the distance between neighboring parallel boundaries (including DBBs and grain boundaries) along the compression axis is measured to characterize deformation banding, as shown in Fig. 8. The error bars in Fig. 8(a) stand for the average band width of boundary

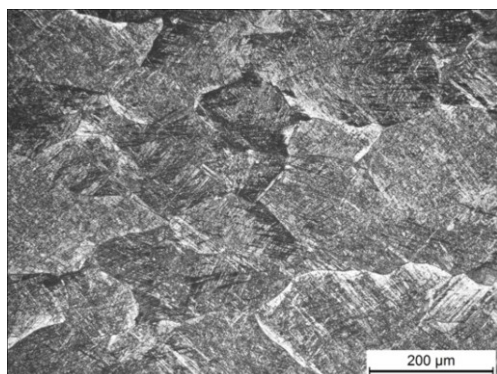


Fig. 7 DDRX at temperature of 1293 K, strain rate of 0.01 s^{-1} and strain of 1.3

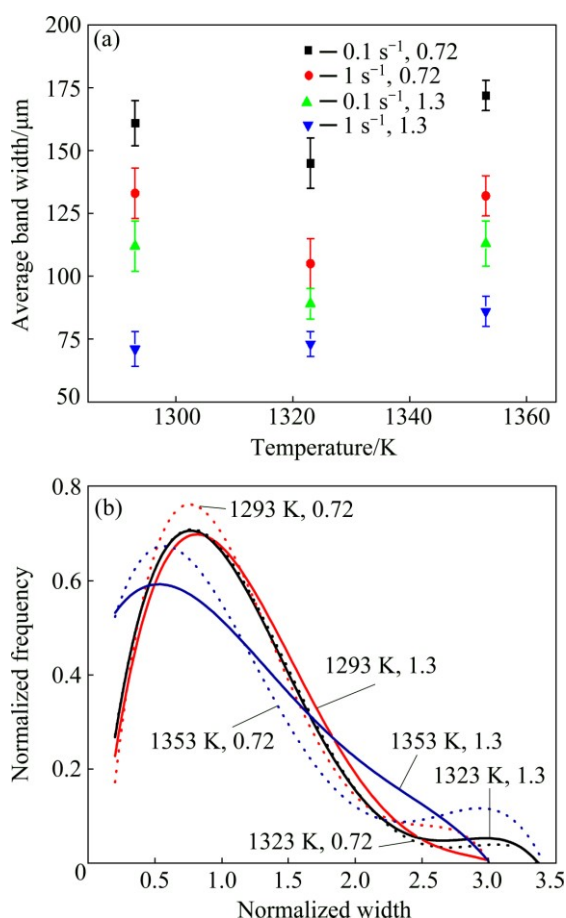


Fig. 8 Band width of boundary intervals after deformation (The initial grain size is $300\text{--}500 \mu\text{m}$): (a) Average band width at different strain rates and strains; (b) Distribution of band width at 1 s^{-1} , different temperatures and strains

intervals measured in two metallographs. Also, the distribution of boundary intervals is measured to characterize the heterogeneity of DBs, of which the normalized width is the specific value between measured band width and average band width in Fig. 8(b). Here, the volume fraction of banded grains is not used because initial grains cannot be distinguished especially at large strain.

Band width decreases with increasing strain rate as expected because the high strain rate can suppress dynamic restoration by other microstructural mechanisms. Band width also decreases with increasing strain. However, considering the geometrical change during compression (the height of specimen at strain of 1.3 is about $2/3$ of that at 0.72), the band width varies little. It is also found that the distribution of band width changes little with increasing strain (Fig. 8(b)). Therefore, it can be deduced that DBs have already formed at strain of 0.72. Additional strain sharpens the DBBs but only leads to slight increase in new DBs. In other words, deformation banding saturates when critical strain is reached.

The band width decreases slightly with increasing temperature and then increases. Commonly, the band width should increase monotonically with increasing temperature as the DB number decreases with increasing temperature [20]. However, it may be easier to obtain sharp DBBs which can be identified in light micrographs, so the measured band width varies little with temperature.

The distribution function of band width suggests that there are some stable grains which are not subdivided at large strain. The number of the stable grains or grain subdivisions increases with increasing temperature as the distribution becomes more uniform. This agrees with the fact that DBs are suppressed at high deformation temperature.

It can be deduced from the measured band width that the number of DBs per grain is small because the band width is about $1/5\text{--}1/7$ of the initial grain size at the strain of 1.3. Assuming homogeneous deformation, the width of pancaked grains is about $2/5$ of the initial size. DB-induced grain subdivision is not significant for a relatively fine initial grain size.

For initially coarse-grained material, the split grains are easier to be identified, so the band width in those grains is measured, as shown in Fig. 9. At the strain of 1.3, most grains in the measured zone produce DBBs. Therefore, the band width is close to the distance between neighboring parallel boundaries defined above. Band width is about $1/10$ of the initial grain size, suggesting that deformation banding is promoted in coarse-grained material. This is in consistence with previous study [20]. Also, the average band width is

close to that for fine-grained material (Fig. 8(a)). Thus, the band width is less dependent on grain size. Similar to fine-grained material, the band width is not sensitive to deformation temperature but decreases sharply with the increase of strain. The band width at strain of 1.3 is about half of that at strain of 0.72. So, only few new observable DBBs are produced due to further increase of strain. This is similar to the result of fine-grained material (Fig. 8).

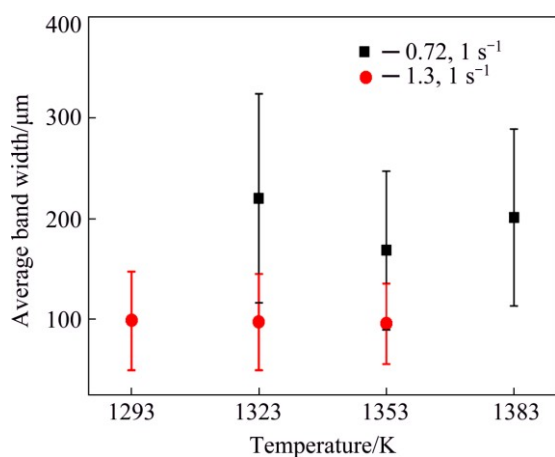


Fig. 9 Measured average band width in subdivided grains at different temperatures (The initial grain size is about 1 mm)

3.4 Heterogeneity of DBs

Deformation banding is related to inhomogeneous deformation of grain interior. It would be suppressed in high temperature deformation. As a result, the formation of observable DBs could be heterogeneous. In low temperature deformation, the whole grain is occupied by plate-like DBs with similar thickness and the DDBs often go through the grain. In this work, however, the observable DBBs are much less and some of them tend to end before reaching the grain boundaries, so the grains are separated into blocks with the variation of thickness. This is more significant at small strain (0.27–0.72), as illustrated by the measured band width in Fig. 9.

On one hand, deformation banding may be suppressed in some grains as it is greatly affected by crystal orientation [20]. On the other hand, observable DBBs are not formed in some grains which have been severely compressed (Fig. 10(a)). This does not mean that DB does not occur in these grains, and there are some grains with large measured band width (Fig. 8(b)). However, DBs can be observed at strain less than 0.3. We also have observed some boundaries inside the grains when the specimen was held for a few seconds after deformation (Fig. 10(b)).

The distance between two boundaries is comparable to the width of deformation band. They may evolve from DDBs with low misorientation, which may not be clearly observed in light micrograph. These boundaries may gradually evolve to HAGBs with further increase of

strain. As a result, more grains are split. This phenomenon only prevails for coarse-grained material, in which the fraction of split grains increases with the increase of strain. For fine-grained material, the width of the pancaked grain gets close to the width of DBs after deformation. As a result, deformation banding is prohibited in the remnant grains.

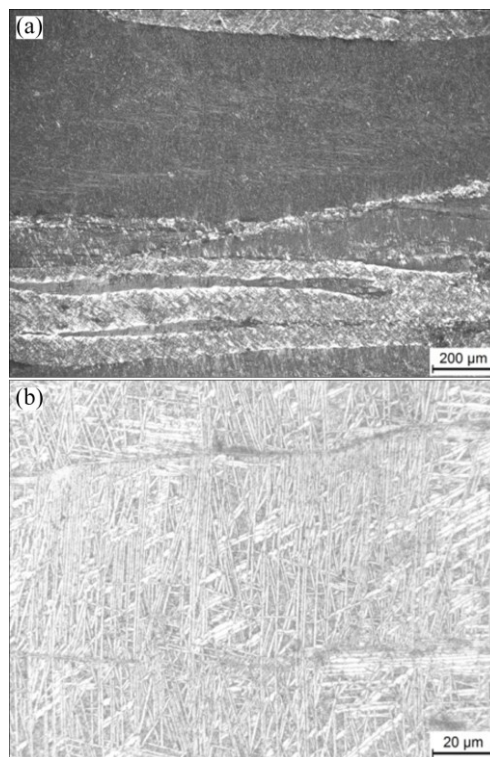


Fig. 10 Heterogeneous formation of DBs: (a) DBs in different grains at temperature of 1323 K, strain rate of 1 s⁻¹ and strain about 1; (b) Suspected boundaries after deformation at 1353 K, 1 s⁻¹, strain of 0.72 and holding for 55 s

3.5 Deformation banding and recrystallization

DDR_X and DBs can appear simultaneously in this work. A typical example is given in Fig. 11(a). Small isolated grains appear at the original grain boundaries, as shown by the red arrows, which are DDR_Xed grains. Meanwhile, DBs are found in the neighboring grains, as shown by the blue arrow. DDR_X is driven by the reduction in stored energy, and DDR_Xed grains nucleate preferentially at the grain boundaries where large inhomogeneous deformation occurs. Both DDR_X and deformation banding tend to reduce the stored energy in hot deformation and can be taken as softening mechanisms, and they are related to the inhomogeneous deformation in grains. With increasing temperature and decreasing strain rate, deformation banding is suppressed while DDR_X is promoted, so they are competing softening mechanisms. DDR_X eliminates the crystal defects in deformation matrix and produces new small

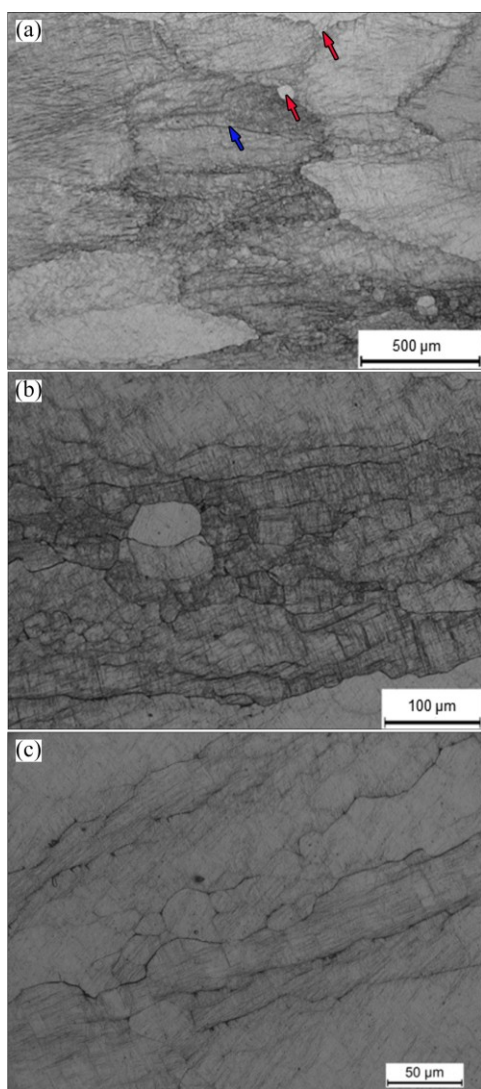


Fig. 11 Optical micrographs of DRX in β working of TA15 alloy deformed at 1453 K, 1 s^{-1} and strain of 0.72: (a) DDRX; (b) CDRX; (c) CDRX grains in chains

grains as well. This would release the hardening caused by increasing number of simultaneously acting slip systems, decrease the stress concentration and coordinate the inhomogeneous deformation. As a result, deformation banding is suppressed to some extent. Meanwhile, deformation banding can reduce the stored energy in deformation matrix and consequently the driving force for DDRX. This phenomenon is more significant at large strain. It is commonly recognized that diffusive DBBs (transition bands) are nucleation sites for recrystallization as the subgrains there have larger misorientation. Thus, deformation banding should promote the nucleation of DDRX. However, DBBs become sharp and smooth at large strain, which greatly prohibit the nucleation of recrystallization. It has been found that post dynamic recrystallization was greatly retarded at large deformation. Therefore, deformation banding can suppress DDRX.

Besides DDRX, CDRX is also reported in titanium alloys [16–18]. In severe plastic deformation (SPD) of aluminum alloy, the formation of CDRX is strongly related to grain subdivision process (micro-shearing banding in their work) [15,26–28]. SAKAI et al [28] has proposed a model for CDRX based on the evolution of MSBs (MSB model) to explain the UFG formation in SPD.

As CDRX grains are firstly formed inside MSBs, they often appear in chains along the original grain boundaries or near the sub-boundaries. In this work, colonies of equiaxed grains in chains are also observed along the β grain boundaries or inside the grains, as shown in Fig. 11(b). Therefore, besides DDRX, CDRX also occurs.

Unlike the UFGs produced in SPD of aluminum alloy (less than $10 \mu\text{m}$), the typical grain size is $20\text{--}30 \mu\text{m}$. The grains are likely to form near or inside the DBBs, as shown in Fig. 11(c). In transition bands, there are substructures to accommodate the orientation change. DBBs consist of volume elements in slab-like parallel sequences with average lattice orientation [20]. They may gradually evolve to isolated grains when the misorientation is large enough. Sakai model [20] can be used to interpret CDRX in this work only when the role of MSB is replaced by transition band. The scale of DB is larger than that of MSB. So, the CDRX grain size is larger in this work. Meanwhile, the misorientation for transition bands increases fast with the increase of strain. CDRX grains can be observed at a relatively small strain.

Instead of fragmentation conducted by DRX, which is the most important grain refinement mechanism in β working of titanium alloy, DBBs can be used to split the coarse grains. In multi-directional forging of austenite steel, HUANG and XU [29] suggested that the DBs intersected with each other, leading to the subdivision of original grains. DBs with large misorientation appear at a relative small strain. As shown in Fig. 5, misorientation angle of DBBs can be above 30° at strain of 1.3. The obtained grain size should be close to the band width (about $100 \mu\text{m}$), which is larger than the CDRXed grain size but close to the DDRXed grain size at low strain rate. However, the required strain would be much smaller than that for full CDRX and comparable to that for full DDRX. This speculation is confirmed by multi-directional forging. Figure 12 gives the microstructures of the large deformation zone in a specimen underwent 2-pass compression. Over half of the deformation matrix is taken by fine equiaxed grains with low aspect ratio (Figs. 12(a) and (b)). The rest (shown by red arrow in Fig. 12(b)) has suspected to be boundaries inside.

This refining method is suitable for small forgings of which multi-direction forging can be finished in short time. For large forgings, SRX may take place during the

high temperature holding between 2 deformation passes or after deformation as the operation time is long. SRX can produce a homogenous microstructure, but the recrystallized grain size would be large.

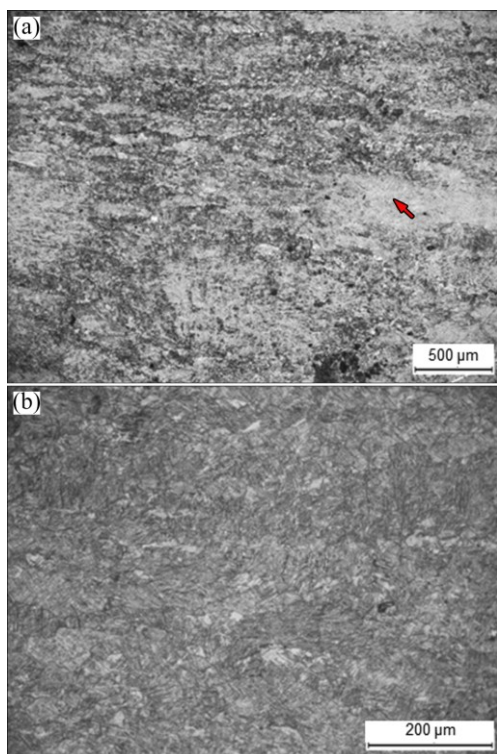


Fig. 12 Low (a) and high (b) magnified optical micrographs of workpiece after 2-pass compression (The specimen was deformed at 1293 K, 1 s^{-1} and strain of 1 in each pass. The micrographs were taken at the center of the specimen)

4 Conclusions

1) Deformation banding occurs up to temperature as high as $0.7T_m$. It is an important reason for flow softening at high strain rate. DBBs may be diffusive or sharp, and the diffusive boundaries may transform to sharp ones with increasing strain.

2) Deformation banding is more significant at high strain rate and large initial grain size. More DBs are produced in coarse-grained material so that the measured width of grain subdivisions varies little from the initial grain size. The number of DBs tends to saturate when critical strain is reached. Further increasing strain sharpens DBBs and increases the misorientation. The formation of HAGBs conducted by DB is heterogeneous inside grains.

3) Deformation banding and DDRX are competing softening mechanisms. Recrystallization is suppressed when sharp DBBs are formed because the smooth boundaries prohibit nucleation. Due to the continuous crystal orientation change in transition bands, diffusive DBBs are the nucleation sites where CDRX starts. Sakai

model can be used to interpret CDRX only when the role of MSB is replaced by transition band.

4) Multi-directional forging can be used to refine the coarse-grained material by producing crossing DBBs. The resulting grain size is close to the DDRX grain size under low strain rate. The required strain is comparable but the deformation speed can be greatly enhanced. This method is potential to refine the microstructure of small forgings.

References

- [1] LÜTJERING G, WILLIAMS J C. Titanium [M]. 2nd ed. Berlin: Springer-Verlag, 2007.
- [2] POLETTI C, GERMAIN L, WARCHOMICKA F, DIKOVITS M, MITSCHE S. Unified description of the softening behavior of beta-metastable and alpha+beta titanium alloys during hot deformation [J]. *Materials Science and Engineering A*, 2016, 651: 280–290.
- [3] WEISS I, SEMIATIN S L. Thermomechanical processing of alpha titanium alloys — An overview [J]. *Materials Science and Engineering A*, 1999, 263: 243–256.
- [4] WEISS I, SEMIATIN S L. Thermomechanical processing of beta titanium alloys—An overview [J]. *Materials Science and Engineering A*, 1998, 243: 16–65.
- [5] BAO Ru-qiang, HUANG Xu, CAO Chun-xiao. Deformation behavior and mechanisms of Ti-1023 alloy [J]. *Transactions of Nonferrous Metals Society of China*, 2006, 16: 274–280.
- [6] DING R, GUO Z X, WILSON A. Microstructural evolution of a Ti-6Al-4V alloy during thermomechanical processing [J]. *Materials Science and Engineering A*, 2002, 327: 233–245.
- [7] DING R, GUO Z X. Microstructural evolution of a Ti-6Al-4V alloy during β -phase processing: Experimental and simulative investigations [J]. *Materials Science and Engineering A*, 2004, 365: 172–179.
- [8] LU Shi-qiang, OUYANG De-lai, CUI Xia, WANG Ke-lu. Dynamic recrystallization behavior of burn resistant titanium alloy Ti-25V-15Cr-0.2Si [J]. *Transactions of Nonferrous Metals Society of China*, 2016, 26: 1003–1010.
- [9] OUYANG De-lai, WANG Ke-lu, CUI Xia. Dynamic recrystallization of Ti-6Al-2Zr-1Mo-1V in β forging process [J]. *Transactions of Nonferrous Metals Society of China*, 2012, 22: 761–767.
- [10] FAN X G, YANG H, GAO P F. Deformation behavior and microstructure evolution in multistage hot working of TA15 titanium alloy: On the role of recrystallization [J]. *Journal of Materials Science*, 2011, 46: 6018–6028.
- [11] FURUHARA T, POORGANJI B, ABE H, MAKI T. Dynamic recovery and recrystallization in titanium alloys by hot deformation [J]. *The Journal of The Minerals, Metals & Materials Society (TMS)*, 2007, 27: 64–67.
- [12] SESHACHARYULU T, MEDEIROS S C, FRAZIER W G, PRASAD Y V R K. Hot working of commercial Ti-6Al-4V with an equiaxed α - β microstructure: Materials modeling considerations [J]. *Materials Science and Engineering A*, 2000, 284: 184–194.
- [13] BALASUBRAHMANYAM V V, PRASAD Y V R K. Deformation behaviour of beta titanium alloy Ti-10V-4.5Fe-1.5Al in hot upset forging [J]. *Materials Science and Engineering A*, 2002, 336: 150–158.
- [14] WANG K L, FU M W, LU S Q, ET A L. Study of the dynamic recrystallization of Ti-6.5Al-3.5Mo-1.5Zr-0.3Si alloy in β -forging process via finite element method modeling and microstructure characterization [J]. *Materials & Design*, 2011, 32: 1283–1291.

- [15] SAKAI T, BELYAKOV A, KAIBYSHEV R, MIURA H, JONAS J J. Dynamic and post-dynamic recrystallization under hot, cold and severe plastic deformation conditions [J]. Progress in Material Science, 2014, 60: 130–207.
- [16] MATSUMOTO H, KITAMURA M, LI Y, KOIZUMI Y, CHIBA A. Hot forging characteristic of Ti-5Al-5V-5Mo-3Cr alloy with single metastable β microstructure [J]. Materials Science and Engineering A, 2014, 611: 337–344.
- [17] DIKOVITS M, POLETTI C, WARCHOMICKA F. Deformation mechanisms in the near- β titanium alloy Ti-55531 [J]. Metallurgical and Materials Transactions A, 2014, 45: 1586–1596.
- [18] TIAN Y X, LI S J, HAO Y L, YANG R. High temperature deformation behavior and microstructure evolution mechanism transformation in Ti2448 alloy [J]. Acta Metallurgica Sinica, 2012, 48: 837–844.
- [19] KUHLMANN-WILSDORF D. Overview No. 131 “regular” deformation bands (DBs) and the LEDS hypothesis [J]. Acta Materialia, 1999, 47: 1697–1712.
- [20] HUMPHREYS F J, HATHERLY M. Recrystallization and related annealing phenomena [M]. 2nd ed. Oxford: Elsevier, 2004.
- [21] LIU Q, HANSEN N. Macroscopic and microscopic subdivision of a cold-rolled aluminium single crystal of cubic orientation [J]. Proceedings of the Royal Society of London A, 1998, 454: 2555–2592.
- [22] SITDIKOV O, SAKAI T, GOLOBORODKO A, MIURA H, KAIBYSHEV R. Grain refinement in coarse-grained 7475 Al alloy during severe hot forging [J]. Philosophical Magazine, 2005, 85: 1159–1175.
- [23] KAIBYSHEV R, SITDIKOV O, GOLOBORODKO A, SAKAI T. Grain refinement in as-cast 7475 aluminum alloy under hot deformation [J]. Materials Science and Engineering A, 2003, 344: 348–356.
- [24] HUGHES D A, HANSEN N. High angle boundaries formed by grain subdivision mechanisms [J]. Acta Materialia, 1997, 45: 3871–3886.
- [25] KUHLMANN-WILSDORF D, MOORE J T, STARKE JR EA, KULKARNI SS. Deformation bands, the LEDS theory, and their importance in texture development: Part I. Previous evidence and new observations [J]. Metallurgical and Materials Transactions A, 1999, 30: 2491–2501.
- [26] SITDIKOV O, SAKAI T, GOLOBORODKO A, MIURA H. Grain fragmentation in a coarse-grained 7475 Al alloy during hot deformation [J]. Scripta Materialia, 2004, 51: 175–179.
- [27] SITDIKOV O, SAKAI T, MIURA H, HAMA C. Temperature effect on fine-grained structure formation in high-strength Al alloy 7475 during hot severe deformation [J]. Materials Science and Engineering A, 2009, 516: 180–188.
- [28] SAKAI T, BELYAKOV A, MIURA H. Ultrafine grain formation in ferritic stainless steel during severe plastic deformation [J]. Metallurgical and Materials Transactions A, 2008, 39: 2206–2214.
- [29] HUANG J, XU Z. Evolution mechanism of grain refinement based on dynamic recrystallization in multiaxially forged austenite [J]. Materials Letters, 2006, 60: 1854–1858.

在 β 锻 TA15 两相钛合金中的变形带

樊晓光, 曾祥, 杨合, 高鹏飞, 孟淼, 左瑞, 雷鹏辉

西北工业大学 材料学院 凝固技术国家重点实验室, 西安 710072

摘要: 为了研究在 β 锻 TA15 两相钛合金中的变形带, 在 Gleeble 3500 热模拟实验机上进行热模拟压缩试验, 同时通过光学显微镜(OM)和电子背散射衍射(EBSD)对显微组织进行研究。研究发现: 在 TA15 钛合金 β 变形中, 变形带在温度高达 $0.7T_m$ (T_m 为熔点)时仍是重要的组织细化机制。变形带的边界可以是尖锐或者连续变化的。尖锐的变形带界面能够阻碍不连续动态再结晶形核, 从而抑制再结晶的发生, 而连续变化的界面是连续动态再结晶产生之处。变形带在高应变速率和初始粗晶组织中更加明显。分裂后的晶粒宽度对应变速率敏感, 但受温度和初始晶粒尺寸影响较小。多向锻造产生交织的变形带可用于细化小型锻件的组织。

关键词: TA15 钛合金; β 锻; 变形带; 晶粒细化; 动态再结晶

(Edited by Wei-ping CHEN)